

# Tracking mood fluctuations with functional network patterns

Nykan Mirchi,<sup>1</sup> Richard F. Betzel,<sup>2</sup> Boris C. Bernhardt,<sup>1</sup> Alain Dagher,<sup>1</sup> and Bratislav Mišić<sup>1</sup>

<sup>1</sup>McConnell Brain Imaging Centre, Montréal Neurological Institute, McGill University, Montréal, QC H3A 2B4, Canada, and <sup>2</sup>Department of Psychological, and Brain Sciences, Indiana University, Bloomington, IN 47405, USA

Correspondence should be addressed to Bratislav Mišić, McConnell Brain Imaging Centre, Montréal Neurological Institute, McGill University, Montréal, QC H3A 2B4, Canada. E-mail: bratislav.misic@mcgill.ca.

## Abstract

Subjective mood is a psychophysiological property that depends on complex interactions among the central and peripheral nervous systems. How network interactions in the brain drive temporal fluctuations in mood is unknown. Here we investigate how functional network configuration relates to mood profiles in a single individual over the course of 1 year. Using data from the 'MyConnectome Project', we construct a comprehensive mapping between resting-state functional connectivity (FC) patterns and subjective mood scales using an associative multivariate technique (partial least squares). We report three principal findings. First, FC patterns reliably tracked daily fluctuations in mood. Second, positive mood was marked by an integrated architecture, with prominent interactions between canonical resting-state networks. Finally, one of the top-ranked nodes in mood-related network reconfiguration was the subgenual anterior cingulate cortex, an area commonly associated with mood regulation and dysregulation. Altogether, these results showcase the utility of highly sampled individual-focused data sets for affective neuroscience.

**Key words:** connectome; mood; deep phenotyping; fMRI; connectivity

## Introduction

The brain's white matter architecture promotes coherent signaling among neuronal populations, enabling perception, cognition and action (Fries, 2015; Avena-Koenigsberger *et al.*, 2018). Non-invasive measurements of electromagnetic and hemodynamic neural activity permit comprehensive mapping of statistical interactions among distributed areas, termed functional connectivity (FC). In the absence of overt sensory stimulation or task demands, brain areas spontaneously synchronize to form networks with specific functional characteristics, termed intrinsic connectivity networks or resting-state networks (RSNs; Damoiseaux *et al.*, 2006; Power *et al.*, 2011; Yeo *et al.*, 2011; Cole

*et al.*, 2014). Recent reports demonstrate that resting FC patterns are heritable (Glahn *et al.*, 2010; Ge *et al.*, 2017) and can even be used to identify individuals, much like a fingerprint (Miranda-Dominguez *et al.*, 2014; Finn *et al.*, 2015). A significant body of work has emerged linking resting FC patterns to individual differences in cognitive performance (Smith *et al.*, 2015; Mišić and Sporns, 2016; Rosenberg *et al.*, 2016).

Much like cognition, subjective affect (here referred to as 'mood') also arises from a complex set of network interactions. A fundamental psychophysiological property, mood depends on distributed signaling throughout the central and peripheral nervous systems, involving interoception, emotional state and memory (Critchley, 2005; Kragel *et al.*, 2018). These complex

Received: 11 April 2018; Revised: 12 November 2018; Accepted: 21 November 2018

© The Author(s) 2018. Published by Oxford University Press.

This is an Open Access article distributed under the terms of the Creative Commons Attribution License (<http://creativecommons.org/licenses/by/4.0/>), which permits unrestricted reuse, distribution, and reproduction in any medium, provided the original work is properly cited.

interactions are conditioned by the underlying anatomical connectivity (Joyce and Barbas, 2018). Altered communication throughout this neural circuit is thought to be the origin of mood disorders such as major depressive disorder (MDD; Berman et al., 2014; Mulders et al., 2015). In the cerebral cortex, mood regulation and dysregulation is associated with several key areas, particularly the subgenual portion of the anterior cingulate cortex (sgACC; Brodmann area 25; Mayberg et al., 1999; Price and Drevets, 2012). The circuit embedding of these areas means that pathological perturbations, such as MDD, manifest at the level of large-scale RSNs, including the salience and default mode networks (Mulders et al., 2015). Indeed, areas such as sgACC and their connected neighbors have been proposed as targets for deep brain stimulation to treat MDD (Mayberg et al., 2005; Fox et al., 2014; but see also Holtzheimer et al., 2017).

Systematically relating mood to distributed FC patterns poses a unique challenge. By definition, mood is dynamic, fluctuating over minutes, hours and days. To statistically relate fluctuations in mood with FC patterns, repeated intra-individual sampling is necessary. A recent landmark data set makes such an investigation possible. In the 'MyConnectome Project', a single individual (a healthy 45-year-old male) was phenotyped over the course of several months (Laumann et al., 2015; Poldrack et al., 2015). Weekly functional magnetic resonance imaging (fMRI) scans were accompanied by self-reported measures of affect [expanded Positive and Negative Affect Schedule (PANAS-X); Watson and Clark, 1999] as well as a comprehensive battery of physiological measurements. To date, two studies have investigated the relation between FC and mood in this context. Shine et al. (2016b) examined the propensity for regions to switch allegiance among large-scale networks within recoding sessions and related this property to self-reported attention. Betzel et al. (2017) investigated a similar within-session flexibility measure in relation to subjective mood ratings and found that greater flexibility was associated with positive mood scales. How daily fluctuations in connectivity track mood and how these connectivity patterns are anatomically organized, remains unknown.

In the present report we apply an associative multivariate technique [partial least squares (PLS); McIntosh and Lobaugh, 2004; McIntosh and Mišić, 2013] to the 'MyConnectome' data set to isolate patterns of functional connections and mood profiles that fluctuate together across time. We then characterize the topological organization of mood-related connectivity patterns and identify their epicenters. Finally, we assess the signature of multiple cognitive and affective systems and how their relative balance is related to positive and negative mood.

## Results

Subjective mood ratings were organized into 13 distinct positive and negative scales as proscribed by Watson and Clark (1999): negative affect, positive affect, fear, hostility, guilt, sadness, joviality, self-assurance, attentiveness, shyness, fatigue, serenity and surprise. fMRI data were pre-processed and parceled into 630 cortical and subcortical regions of interest. FC was defined as a zero-lag linear Pearson correlation between regional blood oxygenation level dependent (BOLD) signal time series. Only sessions that had complete fMRI and mood scales were analyzed (total, 73). The upper triangle of FC correlation matrices was submitted to PLS analysis. A form of reduced-rank linear regression, PLS seeks to maximize the relation between individual functional connections and mood scales in a single multivariate pattern (McIntosh and Mišić, 2013).

## Network configuration tracks mood fluctuations

PLS analysis revealed a statistically significant association between FC and mood across 73 sessions (permuted  $P \approx 0$ ) accounting for 52% of the covariance between connectivity and mood. Figure 1 shows (i) functional connections and (ii) mood scales that contribute most to this pattern. Functional connections are weighted by bootstrap ratios, a measure of reliability (see 'Materials and methods' for details).

Elements (connections or mood scales) weighted with the same sign covary positively, while those with opposite signs covary negatively. In other words, connections with positive weights (red) are associated with greater positive mood (e.g. positive, joviality, self-assurance and attentiveness), while connections with negative weights (blue) are associated with greater negative mood (e.g. negative, guilt, sadness and fatigue). Nodes are arranged by their membership in RSNs derived by Yeo et al. (2011; Figure 1A).

To further illustrate the relation between connectivity and mood, Figure 1C shows fluctuations in individual session scores for both patterns. The scalar scores are calculated by projecting individual session data onto the PLS-derived pattern. They reflect the extent to which a given statistical pattern (e.g. functional network or mood profile) is expressed in a given session. The close correspondence between the network and mood scores suggests that when the participant exhibited network configurations similar to Figure 1A (gray), he was more likely to exhibit the mood pattern in Figure 1B (black;  $r = 0.68$ ).

## Regional contributions to mood-related connectivity

We next investigated the contribution of individual brain regions to the mood-related functional network pattern. Figure 2A shows the mean bootstrap ratio (i.e. network contribution) of all functional connections that a given region participates in. Areas with predominantly positive values, such as precuneus, anterior cingulate cortex and medial orbitofrontal cortex, are more prominent in the global network during positive mood. Conversely, areas with negative values, such as paracentral cortex, lateral prefrontal cortex and visual cortex, feature prominently during negative mood. Figure 2B confirms this intuition, showing the top 5% nodes with the greatest mean negative, positive and absolute bootstrap ratio. We note that the positive mood-related pattern closely resembles the default mode network (Greicius et al., 2003; Fox et al., 2005).

Given the high ranking of sgACC in Figure 2B, and its prominent role in mood disorders (Mayberg et al., 2005; Price and Drevets, 2012; Mulders et al., 2015), we next examine its connectivity fingerprint. Figure 3A shows a positive correlation between sgACC FC strength (FC with other nodes) and the PANAS-X positive mood score ( $r = 0.46$ ;  $P = 3.83 \times 10^{-5}$ ), indicating that overall integration of sgACC was associated with better mood. Note that this relationship is fully expected given the results presented in Figure 2B and cannot be interpreted as an independent discovery (Vul et al., 2009).

Finally, we ask how FC between sgACC and specific large-scale systems relates to mood. Figure 3B shows how mean sgACC-RSN FC correlates with positive mood (circles). While connectivity with some RSNs was associated with greater positive mood, for others the relationship was reversed, suggesting that sgACC integration did not uniformly predict better mood. To assess the statistical significance of this connectivity fingerprint, we also compute correlations between sgACC-RSN connectivity and positive mood under a null model where RSN labels are randomly permuted for all nodes

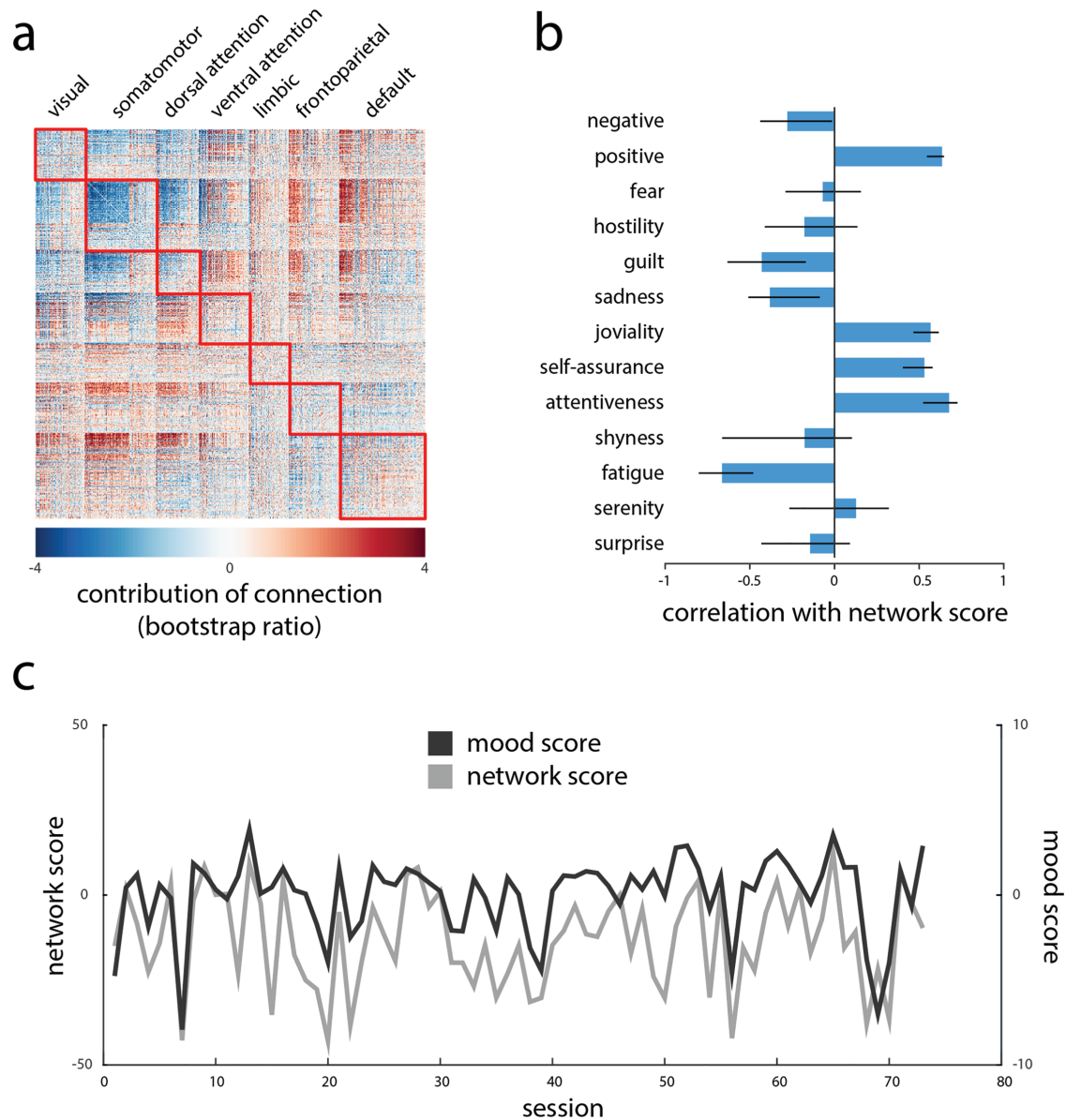


**Fig. 1.** Connectivity patterns track mood patterns. Multivariate PLS analysis was used to isolate patterns of functional connections and PANAS-X mood scales that maximally covary with each other. **(A)** Functional connections that correlate with positive mood (red) and negative mood (blue). Connections are weighted by bootstrap ratios (singular vector weight divided by its bootstrap-estimated standard error). **(B)** Correlations (i.e. loadings) of PANAS-X mood scales with the functional network pattern. Error bars represent bootstrap-estimated 95% CIs. **(C)** Network and behavioral responses or scores are estimated for each individual session by projecting the session data onto the singular vectors. The scores index the extent to which the participant expressed functional patterns and mood patterns shown in **(A)** and **(B)**.

(Figure 3B; red density). When empirical correlations are expressed as z-scores relative to the null distribution, only the negative correlations observed between sgACC and the default mode and frontoparietal networks are statistically significant (Figure 3C; permuted  $P \approx 0$  for both). Altogether, these results demonstrate a complex reconfiguration of sgACC connectivity; positive mood is associated not only with a diffuse, non-specific integration of sgACC with other brain regions but also with a specific decorrelation of sgACC from the default mode and frontoparietal networks.

### Positive mood is associated with network integration

Rearranging brain areas by their membership in RSNs (e.g. Figure 1A) suggests that modular structure may potentially

be associated with mood. To further investigate whether network integration shapes the relationship between connectivity patterns and mood, we partitioned the network into RSNs (Yeo et al., 2011) and stratified functional connections into those connecting areas in the same intrinsic network or different networks.

To assess whether RSN-RSN interactions were statistically significant, we used a label-permuting null model. We randomly permuted RSN labels for each node and recalculated the mean bootstrap ratio for connections within and between RSNs (10 000 repetitions; Mišić et al., 2015; 2016). Figure 4A and B show the mean connection bootstrap ratio for positive mood-related and negative mood-related weights, respectively. The weights are expressed as z-scores relative to the label-permuting null distribution. The resulting figure suggests that positive mood is

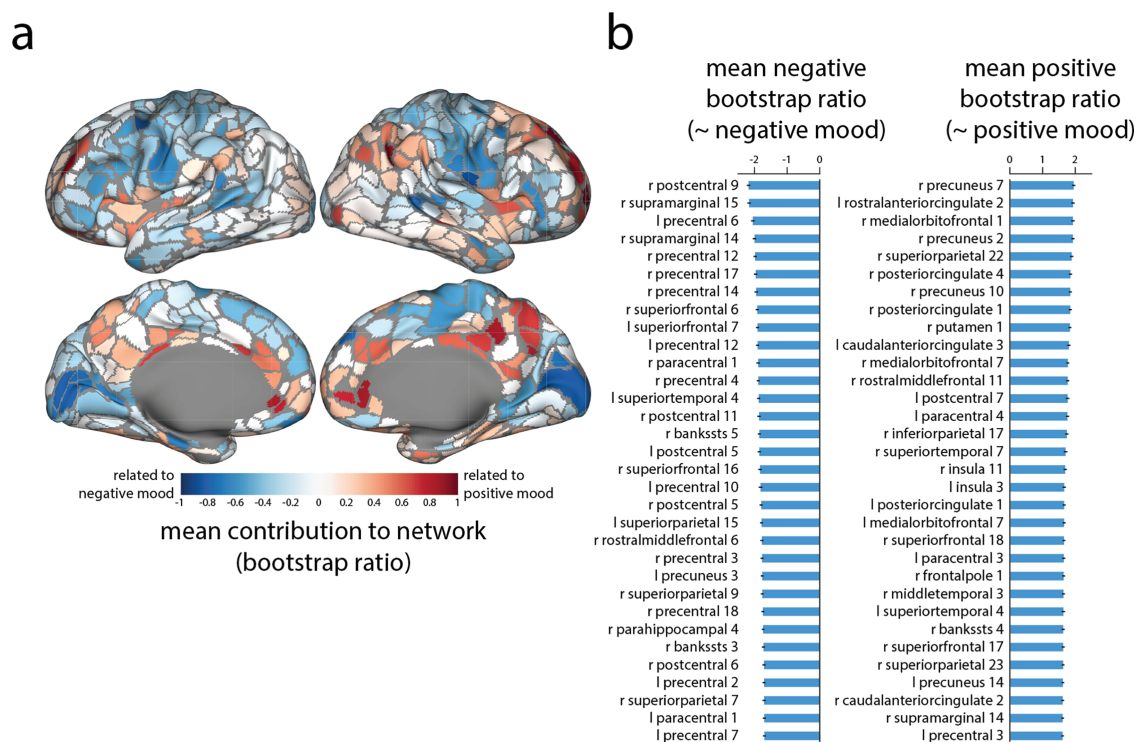


**Fig. 2.** Regional contributions to mood-related network patterns. **(A)** Mean bootstrap ratios of all connections at each region (estimated from Figure 1A). Positive values are associated with more positive mood states, while negative values are associated with negative mood states. **(B)** Top 5% of nodes with the greatest mean negative and positive bootstrap ratio. CIs indicate standard errors.

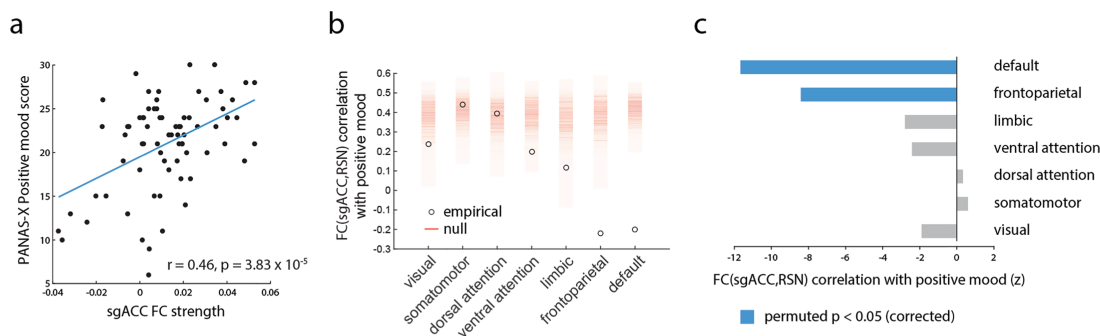


**Fig. 3.** Network embedding of sgACC is associated with mood fluctuations. Based on regional rankings in Figure 2 and prior literature, we investigate the role of sgACC. **(A)** sgACC FC strength (average correlation to other brain areas) correlates with PANAS-X positive mood score across sessions. **(B)** Correlations between positive mood on one hand and FC between sgACC and canonical RSNs on the other. Empirical correlations are displayed as circles; ‘null’ correlations, obtained by permuting RSN labels, are shown as a histogram (red). FC between sgACC and default mode and frontoparietal networks correlates with positive mood significantly less than expected by chance. **(C)** Empirical correlations between FC (sgACC,RSN) and positive mood are shown as z-scores relative to a label-permuting null distribution.

generally associated with between-RSN connectivity, while negative mood is associated with within-RSN connectivity, consistent with Figure 1A.

We next investigated the possibility that network integration contributes to positive mood, while network segregation contributes to negative mood. For each experimental session, we correlated the mean value of within- and between-module connections with the session-specific score on the PLS-derived behavioral pattern, corresponding to positive mood. Greater between-module connectivity was associated with positive mood (Spearman  $r = 0.22$ ;  $P = 0.03$ ; Figure 4C), while greater within-module connectivity was associated with negative mood (Spearman  $r = 0.29$ ;  $P = 6.67 \times 10^{-3}$ ; Figure 4D). As two complementary measures of network segregation, we computed

the modularity and system segregation of FC networks in individual sessions (see ‘Materials and methods’; Newman and Girvan, 2004; Chan et al., 2014). Modularity—the tendency for nodes to connect with other nodes in the same RSN—was associated with negative mood (Figure 4E; Spearman  $r = 0.29$ ;  $P = 0.007$ ). Similarly, system segregation—the normalized difference of within- and between-RSN connectivity—was also associated with negative mood (Figure 4F; Spearman  $r = -0.22$ ;  $P = 0.02$ ).

It is possible that these effects are not module-dependent but rather trivially driven by non-specific fluctuations in network density. To test this hypothesis, we permuted module labels but kept the permuted labels the same across all sessions. We then recalculated the correlations between mood and

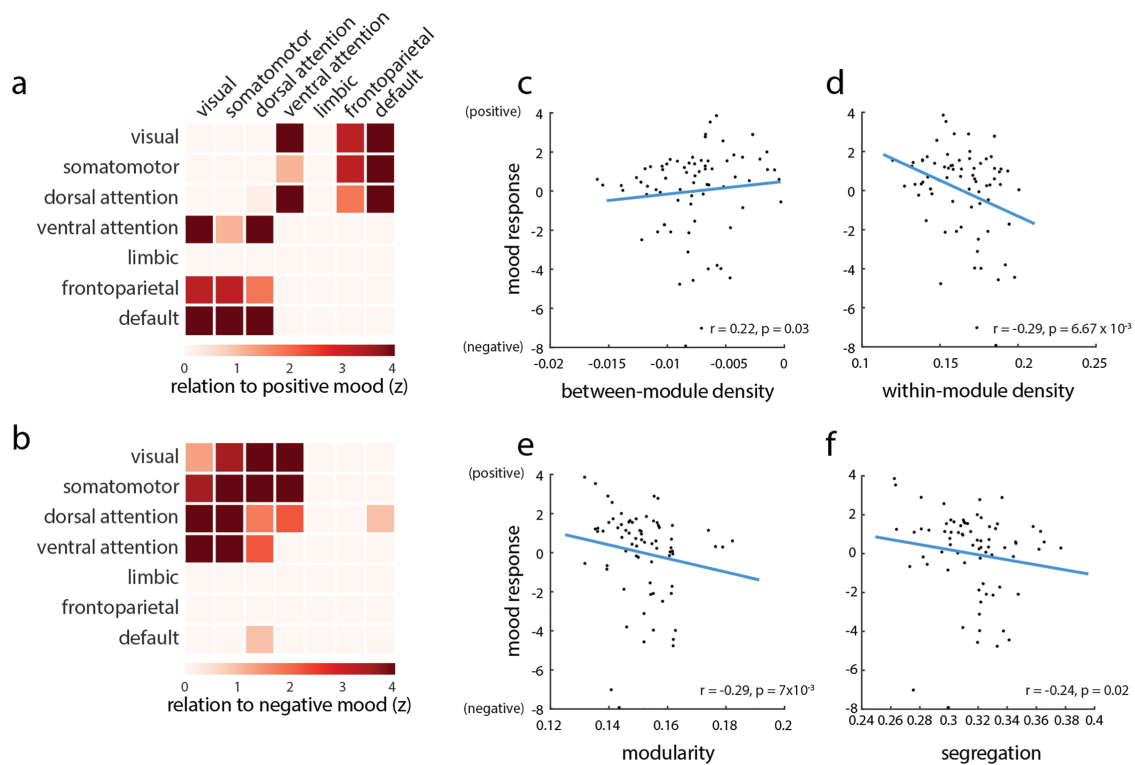


**Fig. 4.** Intrinsic network contributions to mood fluctuations. Bootstrap ratio-weighted functional networks are partitioned according to the RSN assignments reported by Yeo et al. (2011). **(A)** Mean positive bootstrap ratios within and between RSNs, expressed as a z-score relative to a label-permuting null model. High values indicate greater than expected network connectivity during positive mood states. **(B)** The same procedure is performed but focusing on connections related to negative mood. High values indicate greater than expected network connectivity during negative mood states. **(C and F)** Correlating network segregation and integration with behavioral responses (high values are equal to positive mood; low values are equal to negative mood) in individual sessions. Network integration (between-module connectivity) is associated with positive mood, while network segregation (measured by within-module connectivity, modularity and segregation) is associated with negative mood.

within-/between-module density, repeating the procedure 10 000 times. The resulting distribution of correlation coefficients embodies the null hypothesis that density fluctuations drive the observed correlations, as opposed to module assignments. For all four measures (within-module density, between-module density, modularity and segregation), the empirical correlation was significantly greater than expected under the null model (permuted  $P \approx 0$  for all four measures). Altogether, these results indicate that positive mood was broadly associated with greater network integration (higher between-network connectivity) and lower network segregation (higher within-network connectivity).

### Stability of functional and mood patterns

Relating two sets of variables when the number of variables is larger relative to the number of observations poses a risk of overfitting and may result in a model that does not generalize to future observations. Although pattern significance and reliability are assessed by permutation and bootstrapping, respectively, the correlation between brain and behavioral patterns may be optimistic because it is maximized by the analysis.

Here we assess two properties related to stability. First, we assess the stability of the connectivity and behavioral patterns via split-half resampling (Kovacevic et al., 2013; see ‘Materials and methods’ for more details). Briefly, the sample is split into halves and the decomposition is performed on each half separately. Data from one split are then projected onto the left and

right singular vectors (corresponding to the connectivity and mood patterns) calculated from the other split. Pattern stability is quantified as the mean correlation between left/right singular vectors directly calculated from one split and left/right singular vectors calculated by projecting the other split onto the corresponding right/left singular vector. The mean correlation among projected network patterns was  $r = 0.26$  [95% confidence interval (CI): 0.11 0.37], while the correlation among mood patterns was  $r = 0.91$  (95% CI: 0.80 0.94), suggesting that both sets of patterns were stable across splits.

We next assess the out-of-sample correlation between connectivity and mood scores. Following the method described by Rahim et al. (2017), we reran the analysis with 100 randomized train and test splits, where test sets represent 25% of the sample. Test data were projected on the PLS models constructed on the training set. Predicted mood and connectivity scores were then correlated; the resulting mean out-of-sample mood–connectivity correlation was  $r = 0.34$ . The correlation was statistically significant against a permutation test (permuted  $P \approx 0$ ).

### Effects of fasting and lifestyle variables

To facilitate blood tests, the participant did not consume food or caffeine on Tuesday sessions, resulting in a roughly equal split between fasting and non-fasting sessions (39 vs 34). Two previous reports indicated that fasting could alter functional network architecture (Poldrack et al., 2015; Betzel et al., 2017),

suggesting that the present results could be influenced by fasting. To assess this possibility, we directly compared PLS-derived scores on fasting and non-fasting days. Two-sample *t*-tests confirmed significantly different functional network expression on fasting and non-fasting days [ $t(71) = 4.00$ ;  $P = 1.5 \times 10^{-4}$ ]. There was, however, no evidence of significant differences with respect to mood expression [ $t(71) = 1.00$ ;  $P = 0.32$ ]. Importantly, PLS-estimated connectivity and mood pattern scores were correlated on both fasting ( $r = 0.67$ ;  $P = 2.75 \times 10^{-5}$ ) and non-fasting ( $r = 0.74$ ;  $P = 7.13 \times 10^{-7}$ ) days, suggesting that the relation between connectivity and mood was present independent of whether the participant fasted or not. Fisher's test indicated that the two correlation coefficients were not significantly different ( $z = 0.51$ ;  $P = 0.61$ ). Altogether, this suggests that fasting influenced functional network patterns but did not influence mood patterns or the pairing between connectivity and mood patterns.

It is possible that fluctuations in mood and FC depend on a variety of other health and lifestyle variables. To investigate this possibility, we correlated mood scores and network scores separately with variables recorded on evenings before and evenings of the MRI scans. Variables include both subjective and objective measures: same and previous evening subjective measures (alcohol consumption, gut health, psoriasis severity, stress and time spent outdoors), weather (precipitation and lowest and highest temperature) and sleep quality [total sleep time, time in light sleep, deep sleep and rapid eye movement (REM) sleep; Poldrack et al., 2015]. The linear regression analysis revealed no statistically significant associations [ $P > 0.05$  for all comparisons; false discovery rate (FDR) corrected], suggesting that fluctuations in mood and connectivity are unlikely to be explained by these exogenous factors.

## Discussion

In the present report we investigated how FC and mood covary in a single individual over the course of 1 year. We find that fluctuations in mood are reliably tracked by functional network organization. Positive mood was associated with greater integration between canonical intrinsic networks. The sgACC was a highly-ranked node in the isolated network patterns, consistent with its role in rumination and clinical depression.

### Functional network organization and mood

The present results add further evidence that subjective mood is an integrated network property, arising from complex communication patterns throughout the cerebral cortex (Critchley, 2005; Shine et al., 2016b; Betzel et al., 2017). Specifically, mood is thought to arise from a set of polysensory circuits linking interoception, emotion and memory (Critchley, 2005). We find evidence of organized FC network patterns that systematically reconfigure in parallel with mood changes. Positive mood was associated with increased coherence among anterior medial (gACC) and posterior medial (posterior cingulate) structures (Figure 1). More broadly, we find that increased coherence between intrinsic networks (integration) was associated with positive mood, while increased coherence within intrinsic networks (segregation) was associated with negative mood (Figure 4). It is noteworthy that affinity toward integrated states or configurations is also associated with better cognitive performance (Shine et al., 2016a). The present results complement a previous investigation using the 'MyConnectome' data set. Betzel et al. (2017) reported that moment-to-moment

network flexibility was associated with positive mood indices. Our results show that a relationship between network structure and mood can be observed over longer temporal scales as well. Importantly, we find that positive mood is not necessarily associated with random reconfigurations but specifically with a tendency toward less segregated/more integrated states.

These results contribute to a growing literature linking functional network interactions with cognition and affect (Medaglia et al., 2015; Mišić and Sporns, 2016). A number of recent studies have demonstrated that connectivity patterns predict multiple aspects of cognitive performance including fluid intelligence (Smith et al., 2015), cognitive control (Cole et al., 2012), attention (Rosenberg et al., 2016), working memory (Greicius et al., 2003) and learning (Bassett et al., 2015). How functional connections are arranged and rearranged to represent and interact with the external environment remains a key question (Mišić et al., 2014; Zalesky et al., 2014; Shine and Poldrack, 2017).

While ostensibly healthy, the participant's network patterns observed in relation to positive and negative moods mirror those that have been reported in clinical MDD. For example, multiple studies have reported increased FC between sgACC and the default mode network in MDD (Zhou et al., 2010; Davey et al., 2012; de Kwaasteniet et al., 2013), a pattern we observe in relation to decreased positive mood (Figure 3). The increased integration of sgACC effectively changes the configuration of the default mode network in MDD (Greicius et al., 2007). Moreover, treatments such as repetitive transcranial stimulation reduce sgACC default connectivity (Liston et al., 2014; Salomons et al., 2014), consistent with the positive mood-related patterns we observe. Altogether, these potential overlaps suggest that healthy daily fluctuations in mood may be a microcosm of clinical mood disorders.

More generally, the reconfiguration of sgACC connectivity demonstrates how systems-level effects can obscure complex connection 'fingerprints' of individual nodes. In the present analysis we find that general default mode connectivity is associated with positive mood (Figure 2); likewise, mean sgACC connectivity (Figure 3A) is also associated with positive mood. However, their mutual connectivity is anticorrelated with positive mood (Figure 3B and C). In other words, the integration of sgACC and other default regions with the rest of the brain is associated with positive mood, but their mutual connectivity is associated with negative mood. How these complex reconfiguration patterns map onto the heterogeneous connection profile of sgACC remains an exciting open question (Palomero-Gallagher et al., 2018).

### Linking mood and physiology

Although it is tempting to interpret associations between functional network organization and mood fluctuations in purely psychological terms, the present results demonstrate the contribution of physiological variables as well. Specifically, the participant's fasting on approximately half of the scanning sessions had a significant effect on the expression of mood-related connectivity patterns. Although fasting did not influence mood fluctuations or connectivity-mood correlations, the effect of fasting on network expression serves as a reminder that subjective affect may be influenced by a variety of internal and external factors.

A related consideration is the multidimensional nature of subjective affect itself. Modern theories characterize affective experience along at least two distinct dimensions: valence

(the ‘color’ of the experience) and arousal (the intensity of the experience; Feldman, 1995; Anderson et al., 2003). Although the present analysis was designed to allow greater resolution with respect to mood by including all of the PANAS-X categories, it does not permit us to conclusively dissociate valence and arousal. Our results suggest an important role for arousal because PANAS-X categories related to ‘fatigue’ and ‘attentiveness’ loaded highly on the PLS-derived patterns (Figure 1B). This is consistent with the fact that the participant fasted prior to half of the scanning sessions. On fasting days, when the participants consumed neither food nor caffeine, he experienced lower arousal. Altogether, the present results point to a possible role in functional network organization as a method for dissociating neural representations of valence and arousal.

Interestingly, we found no other reliable associations between mood-related network patterns and exogenous lifestyle variables. For instance, network expression did not correlate with previous or same-evening gut health, stress or time spent outdoors. This is surprising given previous demonstrations that even short periods of time spent outdoors (e.g. nature walks) improve cognitive performance, such as working memory (Berman et al., 2008). Lack of association with these variables may therefore suggest that subjective mood is not a simple reflection of environmental and physiological variables but must be considered from the perspective of neural signaling and network-wide interactions.

More generally, our findings open new questions about the physiological and psychological nature of subjective mood. Although we have demonstrated a link with hemodynamic correlations, mood depends on multiple physiological properties that are not accessible via fMRI, including electromagnetic rhythms and neurotransmitter signaling (Castrén, 2005). How proprioceptive and interoceptive signals are interpreted with respect to the external environment and in the context of emotional state remains an open question (Clark et al., 2018). Our results suggest that distributed functional interactions provide a reliable signature of mood fluctuations, but how these functional interactions mediate the integration of sensorimotor and autonomic signals remains to be determined.

### Segregation and integration

Modern theories increasingly emphasize the role of system segregation in cognition and task performance (Shine and Poldrack, 2017; Wig, 2017). Resting-state system segregation, presumably reflecting autonomous processing in specialized circuits, is associated with greater cognitive ability, including episodic memory and fluid processing (Chan et al., 2014; Gu et al., 2015). Likewise, acquisition of automated skills is concomitant with increased segregation (Bassett et al., 2015; Mohr et al., 2016). Conversely, effective task performance, presumably requiring communication among distributed systems, is often associated with decreased segregation, including working memory (Vatansever et al., 2015; Cohen and D’Esposito, 2016; Shine et al., 2016a), cognitive control (Schultz and Cole, 2016; Shine et al., 2016a), emotional/motivational processing (Kinnison et al., 2012) and visuo-spatial attention (Spadone et al., 2015). The present results suggest that a similar segregation–integration framework may apply to subjective affect. We find that daily differences in system segregation track subjective mood ratings, with positive mood associated with reduced segregation among intrinsic networks. While inter-network signaling may directly

contribute to better mood, it may alternatively mediate mood via increased cognitive engagement.

### Methodological considerations

The present results are subject to several methodological considerations and potential limitations. Most importantly, these results are valid only for a single, 45-year-old male individual. Although the observed patterns are concordant with previous literature, further validation is needed in multiple individuals before we can be confident that the observed results will generalize to the rest of the population. We hope that the present report, much like several recent others, will prompt further investigation in single deeply phenotyped individuals (Laumann et al., 2015; Poldrack et al., 2015; Shine et al., 2016b; Betzel et al., 2017; Gordon et al., 2017).

It is important to note that, because there are fewer observations (sessions) than variables (connections), relating connectivity patterns to mood scales is an underdetermined (ill-posed) problem. We have demonstrated the reliability of the results in several ways, including null non-parametric assessment of pattern stability and out-of-sample pairing, but further validation in independently collected data sets is necessary. With the advent of large imaging repositories, directly relating FC patterns to experimental manipulations is becoming an exciting new frontier in human brain mapping (Craddock et al., 2015; Mišić and Sporns, 2016; Smith and Nichols, 2018). Statistical models, such as the one presented here, are still prone to overfitting and external replication is warranted.

### Conclusion

Altogether, our results demonstrate that functional network organization reflects daily fluctuations in subjective mood. Disruption of the intrinsic modular architecture, primarily driven by sgACC and components of the default mode network, is associated with positive mood. These results open exciting new questions about the confluence of proprioceptive and interoceptive signals, how they are mediated by functional neuroanatomy and how this system is disrupted in mood disorders.

### Materials and methods

#### MyConnectome imaging data

The ‘MyConnectome Project’ is a deep phenotyping study of a single individual (male; right-handed; 45 years old) performed over the course of 1 year (Poldrack et al., 2015). All data were downloaded from the project repository (<https://myconnectome.org/wp/data-sharing/>) on 13 April 2016. Brain imaging was performed at fixed times of the day (Tuesdays and Thursdays at 0730 h). Frames were censored (removed) if they had framewise displacement > 0.25 mm or if they were part of contiguous uncensored segments spanning <5 frames. Regressors included whole brain, white matter and ventricular signals and their derivatives, as well as 24 motion regressors derived by Volterra expression. To facilitate subsequent bandpass filtering (0.009–0.08 Hz), data were interpolated over the censored frames by least-squares spectral estimation (Poldrack et al., 2015).

We analyzed the pre-processed, parceled fMRI time series for scan sessions 14–104. The pre-processing procedure is described in detail in (Laumann et al., 2015; Poldrack et al., 2015). The brain was parceled according to a custom partition optimized for the

participant (Laumann et al., 2015) using the procedure developed by Gordon et al. (2014) and Wig et al. (2014). The final parcellation consisted of 616 surface regions and 14 subcortical regions from Freesurfer's subcortical parcellation, for a total of  $N = 630$  regions of interest. Scan sessions were  $\sim 10$  min long and the BOLD signal was sampled with a time to repetition (TR) of 1.16 s, yielding 518 time points per session. FC was defined as a zero-order linear Pearson correlation between regional BOLD time series.

### PANAS-X mood scales

Behavioral data, including self-rated affect, were collected on the same day as the imaging scans. Affective states were measured using the PANAS-X, a 60-item schedule completed using a 0–5 Likert scale (Watson and Clark, 1999). Following Watson and Clark (1999), we distilled the items into 2 general dimension scales (negative affect and positive affect) as well as 11 more specific scales (basic negative emotion scales: fear, hostility, guilt and sadness; basic positive emotion scales: joviality, self-assurance and attentiveness; other affective states: shyness, fatigue, serenity and surprise).

### Partial least squares

PLS analysis was used to relate FC patterns and mood patterns (Wold, 1966; McIntosh and Lobaugh, 2004; Krishnan et al., 2011). The goal of the analysis is to identify weighted patterns of functional connections and mood scales that optimally covary with each other across scanning sessions. A form of reduced rank regression, PLS is closely related to canonical correlation analysis in the sense that both techniques aim to identify weighted mappings between two sets or blocks or variables (Worsley et al., 1997; McIntosh and Mišić, 2013).

Connectivity and mood data were represented as two matrices  $X_{n \times p}$  and  $Y_{n \times q}$ . Both matrices had  $n = 73$  rows corresponding to the scanning sessions. The matrix  $X$  had  $p$  columns, corresponding to unique functional connections. Given  $k$  nodes, there were  $P = k(k-1)/2$  connections. The matrix  $Y$  had  $q$  columns, corresponding to each of the PANAS-X scales. The matrices were standardized column-wise and a correlation matrix ( $X'Y$ ) was computed. The matrix was then subjected to singular value decomposition (SVD; Eckart and Young, 1936)

$$X'Y = USV'. \quad (1)$$

The output of the decomposition are two orthonormal matrices of left and right singular vectors ( $U$  and  $V$ ) and a diagonal matrix of singular values ( $S$ ). The  $i^{\text{th}}$  columns of  $U$  and  $V$  weigh the contribution of individual connections and behaviors, respectively. Collectively, the  $i^{\text{th}}$  left and right singular vectors and singular value constitute a latent variable: a multivariate pattern that weighs the original variables such that they maximally covary with each other. The  $i^{\text{th}}$  singular value is proportional to the total connectivity-behavior covariance accounted for by the latent variable. The effect size associated with a particular latent variable ( $\eta_i$ ) can be estimated as ratio of the squared singular value ( $\sigma$ ) to the sum of all squared singular values:

$$\eta_i = \sigma_i^2 / \sum_j \sigma_j^2. \quad (2)$$

**Permutation tests.** The statistical significance of the overall multivariate pattern was assessed by permutation tests (Nichols and Holmes, 2002). The rows of one of the data matrices ( $X$ ) were randomly permuted, and a connectivity-mood correlation matrix was recomputed. The permuted correlation matrices were subjected to SVD as before, generating a singular value under the null hypothesis that there is no relation between FC and mood. This procedure was repeated 10 000 times to generate a null distribution of singular values. A  $P$ -value was estimated as the proportion of permuted singular values that surpass the original singular value.

**Bootstrap resampling.** Bootstrap resampling was used to estimate the reliability of individual connections and mood scale weights (Efron and Tibshirani, 1986; Milan and Whittaker, 1995). Sessions (i.e. the rows of  $X$  and  $Y$ ) were sampled with replacement, and the resampled data matrices were used to generate correlation matrices that were then subjected to SVD as described above. The procedure was repeated 10 000 times, allowing us to construct a sampling distribution for each individual connection and behavior weight. To identify connections and mood measures that (a) made a large contribution to the overall pattern and (b) were stable across sessions, we calculated the ratio of a variable's weight ( $w_i$ ) to its bootstrap-estimated standard error [ $SE(w_i)$ ], termed 'bootstrap ratio':

$$b_i = w_i / SE(w_i). \quad (3)$$

If the bootstrap distribution is approximately Gaussian, the bootstrap ratio is equivalent to a  $z$ -score (Efron and Tibshirani, 1986). It is important to note that in the present analysis, where observations represent single-subject trials, the estimated sampling distributions yield CIs on fixed effects. As such, stability estimates may be vulnerable to natural or artefactual signal autocorrelation (e.g. due to movement or respiration).

**Split-half resampling.** To assess the generalizability of the estimated patterns, we performed split-half reliability testing (Kovacevic et al., 2013). We randomly split sessions into two halves and calculated separate correlation matrices for each split ( $X'Y_1$  and  $X'Y_2$ ). We then projected each matrix onto the original singular vectors  $U$  and  $V$  to estimate the corresponding singular vectors:

$$\begin{aligned} U_1 &= X'Y_1VS^{-1} & \text{and} & & U_2 &= X'Y_2VS^{-1} \\ V_1 &= X'Y_1US^{-1} & \text{and} & & V_2 &= X'Y_2US^{-1} \end{aligned} \quad (4)$$

Finally, we correlate the projected left and right split-half patterns (i.e.  $U_1$  and  $U_2$ , and  $V_1$  and  $V_2$ ) across 1000 splits. The resulting correlations measure how reliably the FC and behavioral patterns can be paired with one another.

**Cross-validation.** As a final assessment, we estimated the out-of-sample correlation between connectivity and mood scores (Rahim et al., 2017). The analysis was performed on 100 randomized train and test splits, with test sets representing 25% of the sample (19 sessions). Test data were projected on PLS-derived singular vectors, and the resulting test sample scores were correlated with each other. To assess the statistical significance of the correlation coefficient, we performed a

permutation test with 1000 replications. Rows of the FC data matrix  $X$  were randomly permuted, and the procedure for estimating out-of-sample correlations between singular vectors was repeated. A  $P$ -value was estimated as the proportion of correlation coefficients generated for the randomly permuted samples that exceeded the original correlation coefficient.

### Modularity and segregation

Modularity ( $Q$ ) is a commonly used quality function in community detection that quantifies the tendency for groups of nodes to form densely interconnected modules (Newman and Girvan, 2004):

$$Q = \sum_{ij} [w_{ij} - p_{ij}] \delta(c_i, c_j), \quad (5)$$

where  $w_{ij}$  is the observed positive-valued connection weight between nodes  $i$  and  $j$ , while  $p_{ij}$  is the expected connection weight between the nodes. The Kronecker delta function,  $\delta(c_i, c_j)$ , is equal to 1 when nodes  $i$  and  $j$  are assigned to the same community ( $c_i = c_j$ ) and zero otherwise ( $c_i \neq c_j$ ), ensuring that modularity is only computed for pairs of nodes belonging to the same community. The expected connection weight between pairs of nodes is defined according to the standard configuration model, such that

$$p_{ij} = \frac{s_i s_j}{2m}, \quad (6)$$

where  $s_i = \sum_j w_{ij}$  is the strength of node  $i$  and  $m = \sum_{i,j} w_{ij}$  is total weight of all connections in the network. Under this null model, communities are considered to be of high quality if the constituent nodes are more highly correlated with each other than in a randomly rewired network with the same strength distribution and density.

An alternative measure of separation among putative communities is system segregation (Chan et al., 2014). The measure ( $S$ ) is defined as the normalized difference of mean within- and between-community connectivity:

$$S = Z_w - Z_b Z_w, \quad (7)$$

where  $Z_w$  and  $Z_b$  are the mean within- and between-community connection strengths, respectively.

### Funding

This research was supported by the Canada First Research Excellence Fund, awarded to McGill University for the Healthy Brains for Healthy Lives: 1a-DF-1 initiative, Natural Sciences and Engineering Research Council of Canada (01704265 to B.M.) and Fonds de Recherche Québec—Santé: 36767 (chercheur boursier; to B.M.).

### Acknowledgments

The authors would like to thank Estefany Suarez, Golia Shafiei, Ross Markello and Ying-Qiu Zheng for comments and suggestions.

### References

Anderson, A.K., Christoff, K., Stappen, I., et al. (2003). Dissociated neural representations of intensity and valence in human olfaction. *Nature Neuroscience*, *6*(2), 196.

- Avena-Koenigsberger, A., Misisic, B., Sporns, O. (2018). Communication dynamics in complex brain networks. *Nature Reviews Neuroscience*, *19*(1), 17.
- Bassett, D.S., Yang, M., Wymbs, N.F., Grafton, S.T. (2015). Learning-induced autonomy of sensorimotor systems. *Nature Neuroscience*, *18*(5), 744.
- Berman, M.G., Jonides, J., Kaplan, S. (2008). The cognitive benefits of interacting with nature. *Psychological Science*, *19*(12), 1207–12.
- Berman, M.G., Misisic, B., Buschkuhl, M., et al. (2014). Does resting-state connectivity reflect depressive rumination? A tale of two analyses. *NeuroImage*, *103*, 267–79.
- Betz, R.F., Satterthwaite, T.D., Gold, J.I., Bassett, D.S. (2017). Positive affect, surprise, and fatigue are correlates of network flexibility. *Scientific Reports*, *7*, 520.
- Castrén, E. (2005). Is mood chemistry? *Nature Reviews Neuroscience*, *6*(3), 241.
- Chan, M.Y., Park, D.C., Savalia, N.K., Petersen, S.E., Wig, G.S. (2014). Decreased segregation of brain systems across the healthy adult lifespan. *Proceedings of the National Academy of Sciences of the United States of America*, *111*(46), E4997–5006.
- Clark, J.E., Watson, S., Friston, K.J. (2018). What is mood? A computational perspective. *Psychological Medicine*, *48*(14), 2277–2284.
- Cohen, J.R., D'Esposito, M. (2016). The segregation and integration of distinct brain networks and their relationship to cognition. *The Journal of Neuroscience*, *36*(48), 12083–12094.
- Cole, M.W., Yarkoni, T., Repovs, G., Anticevic, A., Braver, T.S. (2012). Global connectivity of prefrontal cortex predicts cognitive control and intelligence. *The Journal of Neuroscience*, *32*(26), 8988–99.
- Cole, M.W., Bassett, D.S., Power, J.D., Braver, T.S., Petersen, S.E. (2014). Intrinsic and task-evoked network architectures of the human brain. *Neuron*, *83*(1), 238–51.
- Craddock, R.C., Tunngaraza, R.L., Milham, M.P. (2015). Connectomics and new approaches for analyzing human brain functional connectivity. *Gigascience*, *4*(1), 13.
- Critchley, H.D. (2005). Neural mechanisms of autonomic, affective, and cognitive integration. *The Journal of Comparative Neurology*, *493*(1), 154–66.
- Damoiseaux, J., Rombouts, S., Barkhof, F., et al. (2006). Consistent resting-state networks across healthy subjects. *Proceedings of the National Academy of Sciences of the United States of America*, *103*(37), 13848–13853.
- Davey, C.G., Harrison, B.J., Yücel, M., Allen, N.B. (2012). Regionally specific alterations in functional connectivity of the anterior cingulate cortex in major depressive disorder. *Psychological Medicine*, *42*(10), 2071–81.
- Eckart, C., Young, G. (1936). The approximation of one matrix by another of lower rank. *Psychometrika*, *1*(3), 211–8.
- Efron, B., Tibshirani, R. (1986). Bootstrap methods for standard errors, confidence intervals, and other measures of statistical accuracy. *Statistical Science*, *1*(1), 54–75.
- Feldman, L.A. (1995). Valence focus and arousal focus: individual differences in the structure of affective experience. *Journal of Personality and Social Psychology*, *69*(1), 153.
- Finn, E.S., Shen, X., Scheinost, D., et al. (2015). Functional connectome fingerprinting: identifying individuals using patterns of brain connectivity. *Nature Neuroscience*, *18*(11), 1664.
- Fox, M.D., Snyder, A.Z., Vincent, J.L., Corbetta, M., Van Essen, D.C., Raichle, M.E. (2005). The human brain is intrinsically organized into dynamic, anticorrelated functional networks. *Proceedings of the National Academy of Sciences of the United States of America*, *102*(27), 9673–8.

- Fox, M.D., Buckner, R.L., Liu, H., Chakravarty, M.M., Lozano, A.M., Pascual-Leone, A. (2014). Resting-state networks link invasive and noninvasive brain stimulation across diverse psychiatric and neurological diseases. *Proceedings of the National Academy of Sciences of the United States of America*, **111**(41), E4367–75.
- Fries, P. (2015). Rhythms for cognition: communication through coherence. *Neuron*, **88**(1), 220–35.
- Ge, T., Holmes, A.J., Buckner, R.L., Smoller, J.W., Sabuncu, M.R. (2017). Heritability analysis with repeat measurements and its application to resting-state functional connectivity. *Proceedings of the National Academy of Sciences of the United States of America*, **114**(21), 5521–6.
- Glahn, D.C., Winkler, A., Kochunov, P., et al. (2010). Genetic control over the resting brain. *Proceedings of the National Academy of Sciences of the United States of America*, **107**(3), 1223–8.
- Gordon, E.M., Laumann, T.O., Adeyemo, B., Huckins, J.F., Kelley, W.M., Petersen, S.E. (2014). Generation and evaluation of a cortical area parcellation from resting-state correlations. *Cerebral Cortex*, **26**(1), 288–303.
- Gordon, E.M., Laumann, T.O., Gilmore, A.W., et al. (2017). Precision functional mapping of individual human brains. *Neuron*, **95**(4), 791–807.
- Greicius, M.D., Krasnow, B., Reiss, A.L., Menon, V. (2003). Functional connectivity in the resting brain: a network analysis of the default mode hypothesis. *Proceedings of the National Academy of Sciences of the United States of America*, **100**(1), 253–8.
- Greicius, M.D., Flores, B.H., Menon, V., et al. (2007). Resting-state functional connectivity in major depression: abnormally increased contributions from subgenual cingulate cortex and thalamus. *Biological Psychiatry*, **62**(5), 429–37.
- Gu, S., Satterthwaite, T.D., Medaglia, J.D., et al. (2015). Emergence of system roles in normative neurodevelopment. *Proceedings of the National Academy of Sciences of the United States of America*, **112**(44), 13681–13686.
- Holtzheimer, P.E., Husain, M.M., Lisanby, S.H., et al. (2017). Subcallosal cingulate deep brain stimulation for treatment-resistant depression: a multisite, randomised, sham-controlled trial. *Lancet Psychiatry*, **4**(11), 839–49.
- Joyce, M.K.P., Barbas, H. (2018). Cortical connections position primate area 25 as a keystone for interoception, emotion, and memory. *The Journal of Neuroscience*, **38**(7), 1677–98.
- Kinnison, J., Padmala, S., Choi, J.M., Pessoa, L. (2012). Network analysis reveals increased integration during emotional and motivational processing. *The Journal of Neuroscience*, **32**(24), 8361–72.
- Kovacevic, N., Abdi, H., Beaton, D., McIntosh, A.R. (2013). Revisiting PLS resampling: comparing significance versus reliability across range of simulations. In: *New Perspectives in Partial Least Squares and Related Methods*, New York, NY, USA: Springer, 159–70.
- Kragel, P.A., Kano, M., Van Oudenhove, L., et al. (2018). Generalizable representations of pain, cognitive control, and negative emotion in medial frontal cortex. *Nature Neuroscience*, **21**(2), 283.
- Krishnan, A., Williams, L.J., McIntosh, A.R., Abdi, H. (2011). Partial least squares (PLS) methods for neuroimaging: a tutorial and review. *NeuroImage*, **56**(2), 455–75.
- de Kwaasteniet, B., Ruhe, E., Caan, M., et al. (2013). Relation between structural and functional connectivity in major depressive disorder. *Biological Psychiatry*, **74**(1), 40–7.
- Laumann, T.O., Gordon, E.M., Adeyemo, B., et al. (2015). Functional system and areal organization of a highly sampled individual human brain. *Neuron*, **87**(3), 657–70.
- Liston, C., Chen, A.C., Zebley, B.D., et al. (2014). Default mode network mechanisms of transcranial magnetic stimulation in depression. *Biological Psychiatry*, **76**(7), 517–26.
- Mayberg, H.S., Liotti, M., Brannan, S.K., et al. (1999). Reciprocal limbic-cortical function and negative mood: converging pet findings in depression and normal sadness. *The American Journal of Psychiatry*, **156**(5), 675–82.
- Mayberg, H.S., Lozano, A.M., Voon, V., et al. (2005). Deep brain stimulation for treatment-resistant depression. *Neuron*, **45**(5), 651–60.
- McIntosh, A.R., Lobaugh, N.J. (2004). Partial least squares analysis of neuroimaging data: applications and advances. *NeuroImage*, **23**, S250–63.
- McIntosh, A.R., Mišić, B. (2013). Multivariate statistical analyses for neuroimaging data. *Annual Review of Psychology*, **64**, 499–525.
- Medaglia, J.D., Lynall, M.E., Bassett, D.S. (2015). Cognitive network neuroscience. *Journal of Cognitive Neuroscience*, **27**(8), 1471–91.
- Milan, L., Whittaker, J. (1995). Application of the parametric bootstrap to models that incorporate a singular value decomposition. *Journal of the Royal Statistical Society. Series C, Applied Statistics*, **44**, 31–49.
- Miranda-Dominguez, O., Mills, B.D., Carpenter, S.D., et al. (2014). Connectotyping: model based fingerprinting of the functional connectome. *PLoS One*, **9**(11), e111048.
- Mišić, B., Sporns, O. (2016). From regions to connections and networks: new bridges between brain and behavior. *Current Opinion in Neurobiology*, **40**, 1–7.
- Mišić, B., Fatima, Z., Askren, M.K., et al. (2014). The functional connectivity landscape of the human brain. *PLoS One*, **9**(10), e111007.
- Mišić, B., Betzel, R.F., Nematzadeh, A., et al. (2015). Cooperative and competitive spreading dynamics on the human connectome. *Neuron*, **86**(6), 1518–29.
- Mišić, B., Betzel, R.F., De Reus, M.A., et al. (2016). Network-level structure-function relationships in human neocortex. *Cerebral Cortex*, **26**(7), 3285–96.
- Mohr, H., Wolfensteller, U., Betzel, R.F., et al. (2016). Integration and segregation of large-scale brain networks during short-term task automatization. *Nature Communications*, **7**, 13217.
- Mulders, P.C., van Eijndhoven, P.F., Schene, A.H., Beckmann, C.F., Tendolkar, I. (2015). Resting-state functional connectivity in major depressive disorder: a review. *Neuroscience and Biobehavioral Reviews*, **56**, 330–44.
- Newman, M.E., Girvan, M. (2004). Finding and evaluating community structure in networks. *Physical Review. E, Statistical, Nonlinear, and Soft Matter Physics*, **69**(2), 026113.
- Nichols, T.E., Holmes, A.P. (2002). Nonparametric permutation tests for functional neuroimaging: a primer with examples. *Human Brain Mapping*, **15**(1), 1–25.
- Palomero-Gallagher, N., Hoffstaedter, F., Mohlberg, H., Eickhoff, S.B., Amunts, K., Zilles, K. (2018). Human pregenual anterior cingulate cortex: structural, functional, and connective heterogeneity. *Cerebral Cortex*, <https://doi.org/10.1093/cercor/bhy124>.
- Poldrack, R.A., Laumann, T.O., Koyejo, O., et al. (2015). Long-term neural and physiological phenotyping of a single human. *Nature Communications*, **6**, 8885.

- Power, J.D., Cohen, A.L., Nelson, S.M., et al. (2011). Functional network organization of the human brain. *Neuron*, *72*(4), 665–78.
- Price, J.L., Drevets, W.C. (2012). Neural circuits underlying the pathophysiology of mood disorders. *Trends in Cognitive Sciences*, *16*(1), 61–71.
- Rahim, M., Thirion, B., Varoquaux, G. (2017). Multi-output predictions from neuroimaging: assessing reduced-rank linear models. In: *2017 International Workshop on Pattern Recognition in Neuroimaging (PRNI)*, Toronto, ON, Canada: IEEE, 1–4.
- Rosenberg, M.D., Finn, E.S., Scheinost, D., et al. (2016). A neuro-marker of sustained attention from whole-brain functional connectivity. *Nature Neuroscience*, *19*(1), 165.
- Salomons, T.V., Dunlop, K., Kennedy, S.H., et al. (2014). Resting-state cortico-thalamic-striatal connectivity predicts response to dorsomedial prefrontal rTMS in major depressive disorder. *Neuropsychopharmacology*, *39*(2), 488.
- Schultz, D.H., Cole, M.W. (2016). Higher intelligence is associated with less task-related brain network reconfiguration. *The Journal of Neuroscience*, *36*(33), 8551–61.
- Shine, J.M., Poldrack, R.A. (2017). Principles of dynamic network reconfiguration across diverse brain states. *NeuroImage*, *180*, 396–405.
- Shine, J.M., Bissett, P.G., Bell, P.T., et al. (2016a). The dynamics of functional brain networks: integrated network states during cognitive task performance. *Neuron*, *92*(2), 544–54.
- Shine, J.M., Koyejo, O., Poldrack, R.A. (2016b). Temporal metastates are associated with differential patterns of time-resolved connectivity, network topology, and attention. *Proceedings of the National Academy of Sciences of the United States of America*, *113*, 9888.
- Smith, S.M., Nichols, T.E. (2018). Statistical challenges in big data human neuroimaging. *Neuron*, *97*(2), 263–8.
- Smith, S.M., Nichols, T.E., Vidaurre, D., et al. (2015). A positive–negative mode of population covariation links brain connectivity, demographics and behavior. *Nature Neuroscience*, *18*(11), 1565.
- Spadone, S., Della Penna, S., Sestieri, C., et al. (2015). Dynamic reorganization of human resting-state networks during visuospatial attention. *Proceedings of the National Academy of Sciences of the United States of America*, *112*, 8112.
- Vatansever, D., Menon, D.K., Manktelow, A.E., Sahakian, B.J., Stamatakis, E.A. (2015). Default mode dynamics for global functional integration. *The Journal of Neuroscience*, *35*(46), 15254–15262.
- Vul, E., Harris, C., Winkielman, P., Pashler, H. (2009). Puzzlingly high correlations in fMRI studies of emotion, personality, and social cognition. *Perspectives on Psychological Science*, *4*(3), 274–90.
- Watson, D., Clark, L.A. (1999). *The PANAS-X: Manual for the Positive and Negative Affect Schedule—Expanded Form*, Iowa City, Iowa, USA: University of Iowa.
- Wig, G.S. (2017). Segregated systems of human brain networks. *Trends in Cognitive Sciences*, *21*, 981–996.
- Wig, G.S., Laumann, T.O., Cohen, A.L., et al. (2014). Parcellating an individual subject's cortical and subcortical brain structures using snowball sampling of resting-state correlations. *Cerebral Cortex*, *24*(8), 2036–54.
- Wold, H. (1966). Estimation of principal components and related models by iterative least squares. In: Krishnaiah, P., editor. *Multivariate Analysis*, Vol. 1, New York: Academic Press, 391–420.
- Worsley, K.J., Poline, J.B., Friston, K.J., Evans, A.C. (1997). Characterizing the response of PET and fMRI data using multivariate linear models. *NeuroImage*, *6*(4), 305–19.
- Yeo, B.T., Krienen, F.M., Sepulcre, J., et al. (2011). The organization of the human cerebral cortex estimated by intrinsic functional connectivity. *Journal of Neurophysiology*, *106*(3), 1125–65.
- Zalesky, A., Fornito, A., Cocchi, L., Gollo, L.L., Breakspear, M. (2014). Time-resolved resting-state brain networks. *Proceedings of the National Academy of Sciences of the United States of America*, *111*(28), 10341–10346.
- Zhou, Y., Yu, C., Zheng, H., et al. (2010). Increased neural resources recruitment in the intrinsic organization in major depression. *Journal of Affective Disorders*, *121*(3), 220–30.